Scientific Research and Essays Vol. 5(12), pp. 1540-1552, 18 June, 2010
Available online at http://www.academicjournals.org/SRE
ISSN 1992-2248 ©2010 Academic Journals

Full Length Research Paper

Multidirectional random wave diffraction in harbours by the placing of submarine pit: A case study

Sung-Duk Kim[1] and Ho Jin Lee[2]*

[1]Department of Civil and Environmental Engineering, Chung-Ang University, 221, Seoul, Korea.
[2]Department of Civil and Environmental Engineering, Colorado State University, Fort Collins, CO 80523, USA.

Accepted 10 May, 2010

The purpose of this study was to estimate the decreasing effects of diffracted wave fields in-and around selected harbours (Kashima and Soma Harbours) including the region of outer breakwater, when a navigation channel is dredged at the vicinity of the harbour entrance. The wave field in the problem is considered to be in a two dimensional plane, and the configuration of the submarine pit breakwater in the sea bed is designated by a single rectangular type. The numerical simulation is performed by using the solution of the boundary integral equation based on the Green function. The incident wave conditions are specified using a discrete form of the Mitsuyasu directional spectrum. Incident wave height is to be decreased in-and behind a pit region by depth discontinuity. It is observed that the wave energy is decreased when a submarine pit has been placed.

Key words: Green function, harbour, navigation channel, Mitsuyasu directional spectrum, pit

INTRODUCTION

When a navigation channel is placed by dredging in the vicinity of a harbour entrance, wave height distribution inside a harbour under multidirectional random wave is put into consideration for planning the layout of facilities. The wave interaction by a depth discontinuity and the scattering at the mouth of the harbour caused by a long pit are important things to consider in the coastal and harbour engineering fields. The interaction of incident waves with a rectangular submarine trench have been studied from the 1960's by Newman (1965); Miles (1967), and in the 1980's by Lee and Ayer (1981); Kirby and Dalrymple (1983). However, in those studies the trench was assumed to be infinitely long and so, the problem was restricted to two-dimension. Later, Williams (1990); McDougal et al. (1996) presented numerical models based on the linearized shallow water wave theory in two horizontal directions for the cases of single and multiple pits, respectively. Takezawa et al. (2000) investigated diffractions for pit breakwater with various configurations, based on the Williams (1990)' method, and presented wave propagation when the pit was dredged at the entrance of a port which was changing the water depth and having refraction, diffraction, and partial-reflection. Briggs et al. (2001) performed experimental and field work at the entrance channel. For the random waves, Kirby (2000) suggested several techniques in Barbers Point Harbour, Hawaii. Reniers et al. (2000) developed computer program for long wave at the pit region. Briggs et al. (2003) studied possibility assessment for deep draft channel design. Those studies were for a train of regular waves propagating over a single pit or multiple pits. The other hand, for the case of beach management dredged pit or channel used (Kennedy et al., 2010; Ravens and Jepsen, 2006; Work et al., 2004).

The present study is about the interaction of waves, which are propagated over a pit with water depth discontinuity, and investigates these waves that instantly affect the inside of a harbour in a multidirectional random wave environment. The wave interaction is connected to three boundary problems which are as follows: the interaction of water depth discontinuity between pit boundaries, the interaction between water depth discontinuity within pit and harbour boundaries, and the interaction between pit boundaries and harbour boundaries. The problem is considered in a two dimensional plane, and the configuration of the submarine pit break - water

*Corresponding author. E-mail: leehojin74@gmail.com.

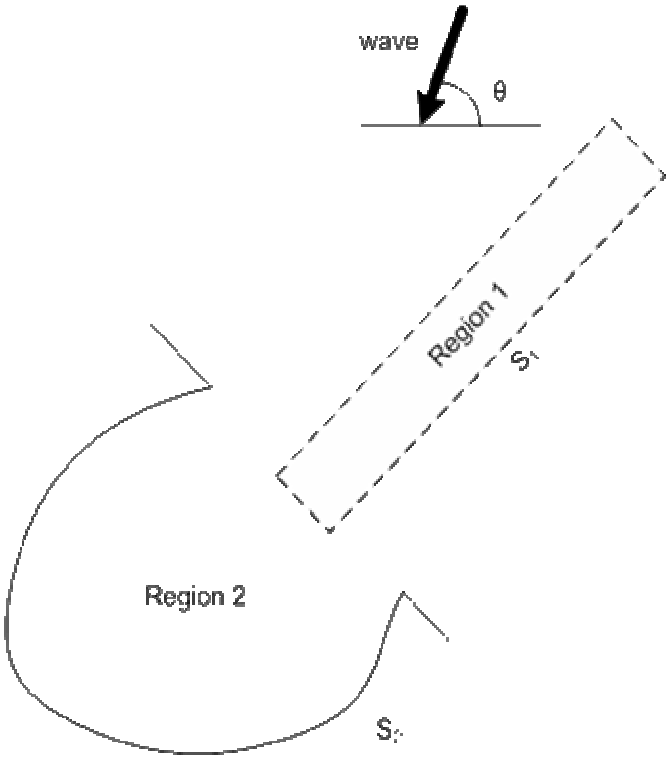

Figure 1. The layout of pit and harbour.

in the sea bed is a single-long rectangular type. The numerical simulation is performed by using the solution of the boundary integral equation based on the Green function.

The incident wave conditions are specified using a discrete form of the Mitsuyasu directional spectrum. For investigating the decreasing effects of diffracted wave fields in a harbour, two kinds of harbours (Kashima and Soma harbours) in Japan were selected. The present study can provide information to design the dredge line of a harbour entrance in real coastal construction. It is then possible to estimate the management cost of a harbour. Furthermore, multidirectional random wave model can be effectively utilized to forecast, with excellent accuracy, of the wave height in-and around the harbour.

THEORETICAL REVIEW

The detail of the theoretical background has been depicted in the paper of Kim (2007). The geometry of the problem is presented in Figure 1. The boundary regions are represented by S_1 (pit boundary line) and S_2 (harbour boundary line), respectively. The fluid is taken to be inviscid and incompressible, and the flow irrotational. It is then assumed that the fluid motion may be described in terms of velocity potential $\phi(x, y, z, t) = \Phi(x, y, z)e^{-i\omega t}$. This potential must satisfy Laplace's equation, $\nabla^2\Phi = 0$. It is subject to the usual boundary conditions on the free surface and seabed, and the solution of velocity potential can be given in the flowing forms.

$$\Phi_1(x,y,z) = \frac{ga}{\sigma} f_1(x,y) \frac{\cosh[k_1(z+d)]}{\cosh(k_1 d)} \quad \text{; Region 1} \tag{1}$$

$$\Phi_2(x,y,z) = \frac{ga}{\sigma} f_2(x,y) \frac{\cosh[k_2(z+h)]}{\cosh(k_2 h)} \quad \text{; Region 2} \tag{2}$$

where, a is the incident wave amplitude, d is the water depth within the pit, h is the water depth of the fluid region (in- and around harbour) beyond the pit region, f_j (j =1, 2) is the wave function, subscript 1 represents the pit region, subscript 2 represents the region without the pit, and the wave numbers k_j (j =1, 2) are defined by

$$\omega^2 = gk_1 \tanh(k_1 d) \quad \text{; Region 1} \tag{3}$$

$$\omega^2 = gk_2 \tanh(k_2 h) \quad \text{; Region 2} \tag{4}$$

Where, ω is angular frequency and g is the gravitational acceleration. The wave function can be described in the following form.

$$f(x,y)_j = f_{ij}(x,y) + f_{rj}(x,y) + f_s(x,y) \quad j=1, 2 \tag{5}$$

$$f_{ij}(x, y) = -ie^{ik_j(x\cos\theta + y\sin\theta)} \quad j=1, 2 \tag{6}$$

$$f_{rj}(x, y) = -ie^{ik_j(x\cos\theta - y\sin\theta)} \quad j=1, 2 \tag{7}$$

Where, f_i is the incident wave function, f_r is the reflective wave function, and f_s is the scattered wave function. $f_s(x, y)$ should be satisfied by the Helmholtz equation.

$$\frac{\partial^2 f_s}{\partial x^2} + \frac{\partial^2 f_s}{\partial y^2} + k_j^2 f_s = 0 \quad j=1, 2 \tag{8}$$

Continuity of mass flux and pressure across the fluid interface between the interior pit region (S_1) and the exterior pit region and harbour region (S_2) requires the following conditions to be satisfied:

$$d\frac{\partial f_1}{\partial n} = h\frac{\partial f_2}{\partial n} \quad \text{on } S_1 \tag{9}$$

$$\phi_1 = \phi_2 \quad \text{on } S_1 \tag{10}$$

Finally, the scattered component of the fluid potential is subjected

to a radiation or far-field boundary condition at large radial distances r, which may be written as

$$\lim_{r\to\infty}\sqrt{r}\left(\frac{\partial f_s}{\partial r}-ik_j f_s\right)=0 \quad ; \ j=1, 2 \tag{11}$$

The boundary conditions at the S_1 and S_2 can express the following:

(i) Without pit

$$\frac{\partial f}{\partial n}=0 \ , \ \frac{\partial f_s}{\partial n}=-\left(\frac{\partial f_i}{\partial n}+\frac{\partial f_r}{\partial n}\right) \quad \text{on } S_2 \tag{12}$$

(ii) With pit

$$\frac{\partial f}{\partial n}=0 \ \text{ and equation (9), } \ \frac{\partial f_s}{\partial n}=-\frac{h}{d}\left(\frac{\partial f_i}{\partial n}\right) \quad \text{on } S_1 \tag{13}$$

$$\frac{\partial f}{\partial n}=0 \ \text{ and equation (9), } \ \frac{\partial f_s}{\partial n}=-\frac{h}{d}\left(\frac{\partial f_i}{\partial n}+\frac{\partial f_r}{\partial n}\right) \quad \text{on } S_2 \tag{14}$$

Applying Green's second identity to $f_s(x,y)$ with considering partial reflection (K_r) and extending to full regions, boundary integral equations can be yielded as without pit (Equation. (15)) and with pit (Equation (16)), respectively.

$$f_s(x,y)=-\int_{S_2}\left[f_s(\xi,\eta)\cdot\frac{\partial}{\partial n}\left(-\frac{1}{2}iH_0^{(1)}(k_2R)\right)+K_r\left(-\frac{1}{2}iH_0^{(1)}(k_2R)\right)\cdot\left(\frac{\partial f_{i_2}}{\partial n}+\frac{\partial f_{r_2}}{\partial n}\right)\right]ds \tag{15}$$

$$f_s(x,y)=-\int_{S_1}\left[f_s(\xi,\eta)\cdot\frac{\partial}{\partial n}\left(-\frac{1}{2}iH_0^{(1)}(k_1R)\right)+\frac{h}{d}\left(-\frac{1}{2}iH_0^{(1)}(k_1R)\right)\cdot\left(\frac{\partial f_{i_1}}{\partial n}\right)\right]ds$$
$$-\int_{S_2}\left[f_s(\xi,\eta)\cdot\frac{\partial}{\partial n}\left(-\frac{1}{2}iH_0^{(1)}(k_2R)\right)+K_r\left(-\frac{1}{2}iH_0^{(1)}(k_2R)\right)\cdot\frac{h}{d}\cdot\left(\frac{\partial f_{i_2}}{\partial n}+\frac{\partial f_{r_2}}{\partial n}\right)\right]ds \tag{16}$$

where, (ξ,η) are the coordinates of the point on the boundary (S_1 , S_2) , (x,y) are the coordinates of the arbitrary point in the Region 1 and 2, n is the normal direction to S , $H_0^{(1)}$ is the Hankel function of the first kind of order zero, and $R^2=(x-\xi)^2+(y-\eta)^2$.

NUMERICAL PROCEDURES

A computer program has been developed to implement the above theory for wave diffraction in harbours by submarine pit. The boundaries S_1 and S_2 were divided by infinitesimal elements of M and N. Discretizing Equation (15) and (16), it can be written as

$$f_s(x,y)=-\sum_{j=1}^{N}\left[f_s(\xi_j,\eta_j)\cdot\overline{B}_{ij}+K_rB_{ij}(\overline{f_i}+\overline{f_r})\right]$$
i=1,2,…,*N* (17)

$$f_s(x,y)=-\sum_{j=1}^{M}\left[f_s(\xi_j,\eta_j)\cdot\overline{A}_{ij}+h/d\cdot A_{ij}(\hat{f}_i)\right]-\sum_{j=M+1}^{M+N}\left[f_s(\xi_j,\eta_j)\cdot\overline{B}_{ij}+K_rB_{ij}\cdot h/d\cdot(\hat{f}_i+\hat{f}_r\right]$$
i=1,2,…*M*…*M+N* (18)

where,

$$\overline{f}_i=\frac{\partial f_i}{k_2\partial n} \ , \ \overline{f}_r=\frac{\partial f_r}{k_2\partial n} \ , \ \hat{f}_i=\frac{\partial f_i}{k_1\partial n} \ , \ \hat{f}_r=\frac{\partial f_r}{k_1\partial n} \tag{19}$$

$$A_{ij}=\int_{\Delta S_j}\left(-\frac{1}{2}iH_o^{(1)}(k_1r)\right)k_1ds=-\frac{1}{2}H_o^{(1)}(k_1r)k_1\Delta S_j$$
($i\neq j$) (20)

$$=\frac{1}{\pi}\left(0.5772-1+\log\frac{k_1\Delta S_i}{4}-i\frac{\pi}{2}\right)k_1\Delta S_i$$
($i=j$)

$$\overline{A}_{ij}=\int_{\Delta S_j}\frac{\partial}{\partial n}\left(-\frac{1}{2}iH_o^{(1)}(k_1r)\right)ds=-\frac{1}{2}iH_o^{(1)}(k$$
$$I_o^{(1)}(k_1r)\cdot\left(\frac{\xi_j-\xi_i}{r}k_1\Delta\eta_j-\frac{\eta_j-\eta_i}{r}k_1\Delta\xi_j\right)$$

$$=\frac{1}{2\pi}(\xi\Delta S-\eta\Delta S)\Delta S_i$$
($i=j$)

$$B_{ij}=\int_{\Delta S_j}\left(-\frac{1}{2}iH_o^{(1)}(k_2r)\right)k_2ds=-\frac{1}{2}H_o^{(1)}(k_2r)k_2\Delta S_j$$
($i\neq j$) (22)

$$=\frac{1}{\pi}\left(0.5772-1+\log\frac{k_2\Delta S_i}{4}-i\frac{\pi}{2}\right)k_2\Delta S_i$$
($i=j$)

$$\overline{B_{ij}}=\int_{\Delta S_j}\frac{\partial}{\partial n}\left(-\frac{1}{2}iH_o^{(1)}(k_2r)\right)ds$$
$$=-\frac{1}{2}iH_o^{(1)}(k_2r)\cdot\left(\frac{\xi_j-\xi_i}{r}k_2\Delta\eta_j-\frac{\eta_j-\eta_i}{r}k_2\Delta\xi_j\right) \tag{23}$$

$$= \frac{1}{2\pi}(\xi \Delta S - \eta \Delta S)\Delta S_i \quad (i = j)$$

$$\overline{f_i} = \frac{\Delta\xi_j \sin\theta - \Delta\eta_j \cos\theta}{\Delta S_j} \cdot e^{-ik_2(\xi_j \cos\theta + \eta_j \sin\theta)} \tag{24}$$

$$\overline{f_r} = \frac{-\Delta\xi_j \sin\theta - \Delta\eta_j \cos\theta}{\Delta S_j} \cdot e^{-ik_2(\xi_j \cos\theta + \eta_j \sin\theta)} \tag{25}$$

$$\hat{f}_i = \frac{\Delta\xi_j \sin\theta - \Delta\eta_j \cos\theta}{\Delta S_j} \cdot e^{-ik_1(\xi_j \cos\theta + \eta_j \sin\theta)} \tag{26}$$

$$\hat{f}_r = \frac{-\Delta\xi_j \sin\theta - \Delta\eta_j \cos\theta}{\Delta S_j} \cdot e^{-ik_1(\xi_j \cos\theta + \eta_j \sin\theta)} \tag{27}$$

MULTIDIRECTIONAL RANDOM WAVE

The regular wave diffraction solution stated above may be extended to a random wave environment using the superposition method. A general form of directional wave spectrum, $S(f,\theta)$, we have $S(f,\theta) = S(f)G(f,\theta)$ in which $S(f)$ is a unidirectional frequency spectrum and $G(f,\theta)$ is a wave directional spreading function. A modified Mitsuyasu spectrum (Mitsuyasu, 1970) is adopted for $S(f)$, is defined in the following form,

$$S(f) = 0.258\frac{H_{1/3}^2}{T_{1/3}^4} f^{-5} \exp\{-1.03(T_{1/3}f)^{-4}\} \tag{28}$$

in which $H_{1/3}$ and $T_{1/3}$ are the significant wave height and period, respectively. The form for the wave directional spreading function $G(f,\theta)$ is due to Mitsuyasu et al. (1975) and is derived from field data obtained from a clover-type buoy,

$$G(f,\theta) = \frac{1}{\pi} 2^{2s-1} \frac{\Gamma^2(s+1)}{\Gamma(2s+1)} \cos^{2s}\frac{\theta}{2} \tag{29}$$

where, $\Gamma(s)$ is the Gamma function and *s* is a wave directional concentration parameter, which can be determined from

$$s = \begin{cases} s_{\max}\left(\frac{f}{f_p}\right)^{-2.5} & for \quad f > f_p \\ s_{\max}\left(\frac{f}{f_p}\right)^{5} & for \quad f \le f_p \end{cases} \tag{30}$$

in which fp is the wave peak frequency, given by $f_p = 1/(1.05T_{1/3})$. Goda et al. (1985) gave the mean value of s_{max} as 10 for wind waves (broad directional spread) and 75 for swells with a long decay distance (narrow directional spread). In numerical applications, the incident wave spectrum must be discretized into a finite number of wave components in order to obtain the diffracted wave spectrum. An adequate discretization in both frequency and direction is essential to obtain meaningful results. In the present work, the number of component frequencies will be denoted by *N* while the number of wave directions will be denoted by *M*. If the frequency range is discretized so that each frequency band has equal energy, then the central frequency fn in the n^{th} section is given by

$$f_n = \frac{1}{0.9T_{1/3}} \sqrt{2.9124N\left[erf\left(\sqrt{2\ln\left(\frac{N}{n-1}\right)}\right) - Erf\left(\sqrt{2\ln\left(\frac{N}{n}\right)}\right)\right]} \tag{31}$$

where, *erf*() is the error function. The frequency spectrum $S^D(\mathbf{x}, f)$ of $\eta^D(\mathbf{x},t)$ can be expressed as

$$S^D(\mathbf{x}, f_n) = \int_{\theta_{\min}}^{\theta_{\max}} S(f_n,\theta) K_d^2(\mathbf{x}, f_n, \theta) d\theta \tag{15}$$

where, $K_d(\mathbf{x}, f, \theta)$ is the diffraction coefficient for a wave component of frequency f_n, propagating in the direction θ. The significant wave heights for incident waves and diffracted waves are defined as (Goda, 1985).

$$(H_{1/3})_I = 4.0\sqrt{(m_o)_I} \tag{32a}$$

$$(H_{1/3})_D = 4.0\sqrt{(m_o)_D} \tag{32b}$$

Where,

$$(m_o)_I = \int_0^{\infty} \int_{\theta_{\min}}^{\theta_{\max}} S(f,\theta) d\theta df \tag{33a}$$

$$(m_o)_D = \int_0^{\infty} \int_{\theta_{\min}}^{\theta_{\max}} S^D(f_n,\theta) d\theta df_n \tag{33b}$$

Finally, in a random wave environment, a diffraction coefficient, K, may be computed using the following equation

$$K = \left|\frac{(H_{1/3})_D}{(H_{1/3})_I}\right| \tag{34}$$

RESULTS AND ANALYSIS

A computer program has been developed to implement the above theory for random wave diffraction in a harbour by a long submarine pit. The present numerical model can study the wave height distributions inside the

Figure 2. The location and layout of the selected harbour.

harbours, which are Kashima and Soma harbour with pit or without pit, respectively. The conditions of calculation for Soma harbour are defined as wave period $T = T_{1/3} = 8.0s$, water depth inside harbour $h = 13m$, water depth within pit $d = 26m$, incident wave angle $\theta = \theta_R = 100^\circ$, and $s_{\max} = 25$. The two kinds of pits are dredged at the entrance of the harbour, and one is horizontal direction with width $B_2 = 50m$ and length $L_2 = 400m$, and the other is oblique direction with width $B_2 = 70m$ and length $L_2 = 390m$, respectively. The conditions of calculation for Kashima harbour are defined as wave period $T = T_{1/3} = 10.0s$, water depth inside harbour $h = 10m$, water depth within pit $d = 20m$, incident wave angle $\theta = \theta_R = 85^\circ$, and $s_{\max} = 25$. The pit is dredged at the entrance of the harbour with width $B_2 = 110m$ and length $L_2 = 1200m$. Figure 2 shows the location and layout of the selected harbours.

Validation of the numerical model

Verification of this study is carried out by simulation regular wave diffraction in harbour with submarine pit. The harbour geometry and the layout of a submarine pit outside of harbour are show in Figure 3. Saito et al. (1993) carried out a series of hydraulic model tests to obtain the wave height distribution in this harbour without considering the effect of a submarine pit. Figure 3 shows a comparison of the results in four lines for the diffraction coefficient of regular waves obtained by the present numerical model and experimental data of Saito et al. (1993), in case of the only left side revetment of harbour with partial reflection boundary. In a comparison of line A - A' and B - B', the experimental value and present numerical value can be seen comparatively good agreement. In a comparison of line X - X', the numerical value and the experimental value are good agreement beside at the vicinity of 6 and 8 m (x-coordinate). In a comparison of line Y - Y', the experimental value and present numerical value can be seen satisfactory agreement beside at the 8 ~ 10 m (x-coordinate).

Analysis of regular waves

Figure 4 shows the results for the diffraction coefficient of regular waves in Soma harbour obtained by the present numerical model. For the case without the pit in Figure 4a, diffracted wave by breakwater occurs with wave superposition. Wave height is high and these high waves propagate into the harbour. For the case of offshore pit in Figure 4b, wave propagates over the pit and the reduction of wave height is shown. Again these waves propagate into the harbour and the wave height is reduced. As for this case, wave height reduction due to pit can be estimated to be 34 ~ 50%. For the case of entrance pit in Figure 4c, the wave height reduction at the entrance of the harbour is shown to be the largest. It means that this entrance pit can help ensure the safety of navigating a large ship.

Figure 5 displays the three dimensional diffraction diagram for regular waves in Soma harbour. For the case without the pit in Figure 5a, when waves propagate and face the breakwater, the wave crest is high and it creates high wave heights inside the harbour. In the case of the entrance pit in Figure 5b, wave height inside the harbour is reduced by the discontinuity of water depth in the pit region.

Figure 6 shows the results for the diffraction coefficient

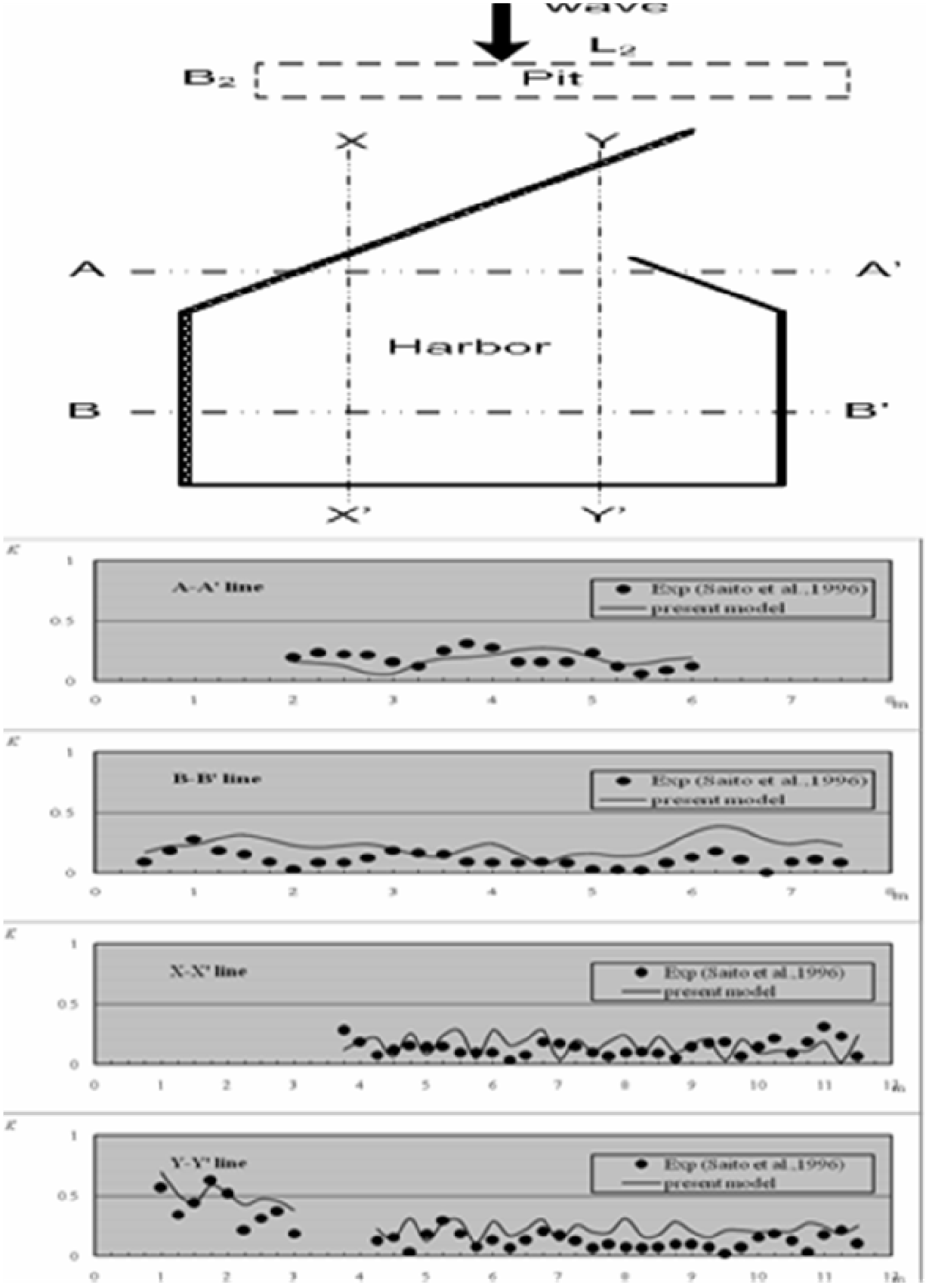

Figure 3. Comparison of diffraction coefficients in a harbor with partial-reflecting boundary.

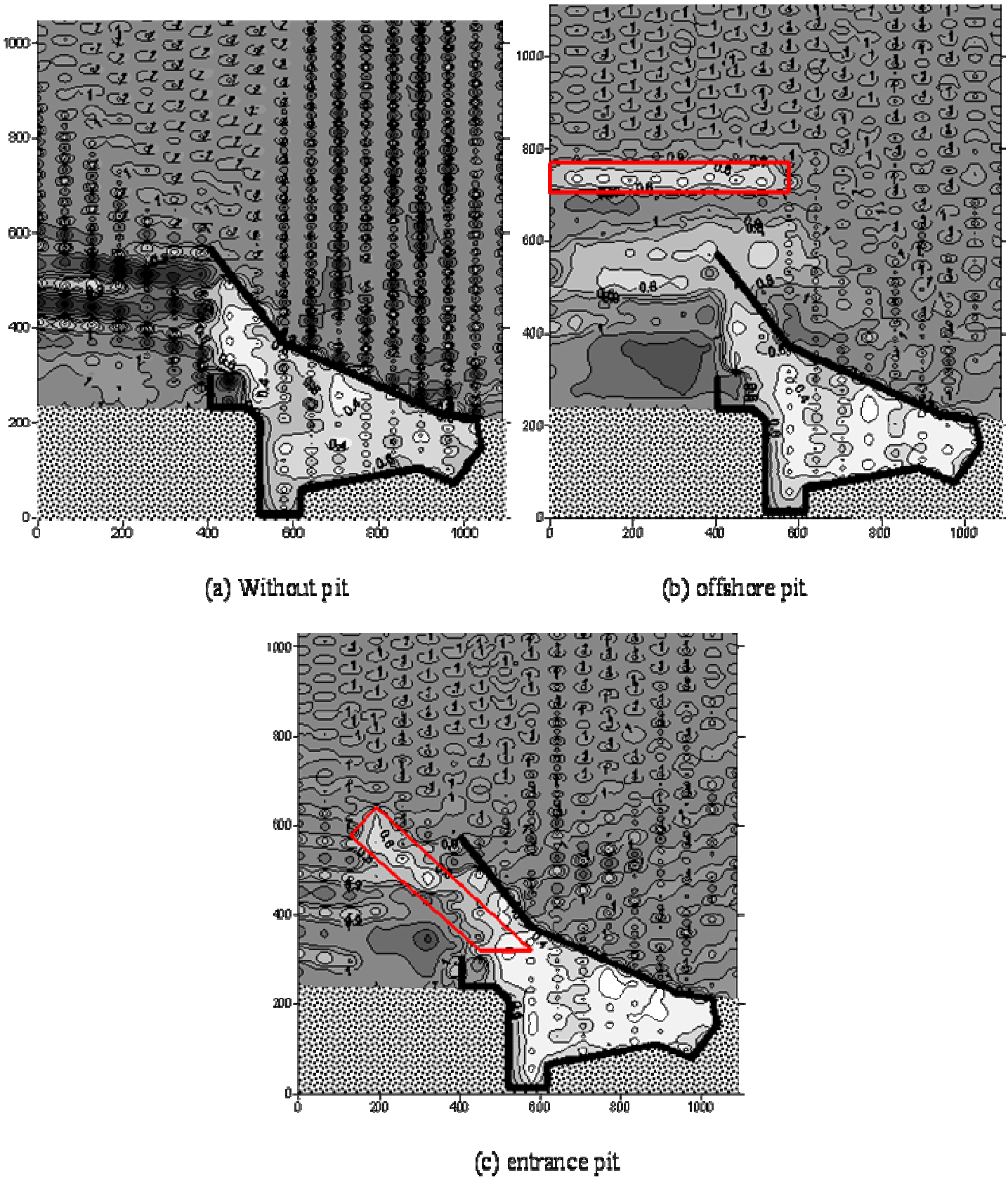

Figure 4. The diffraction contour plots in Soma harbor for regular waves.

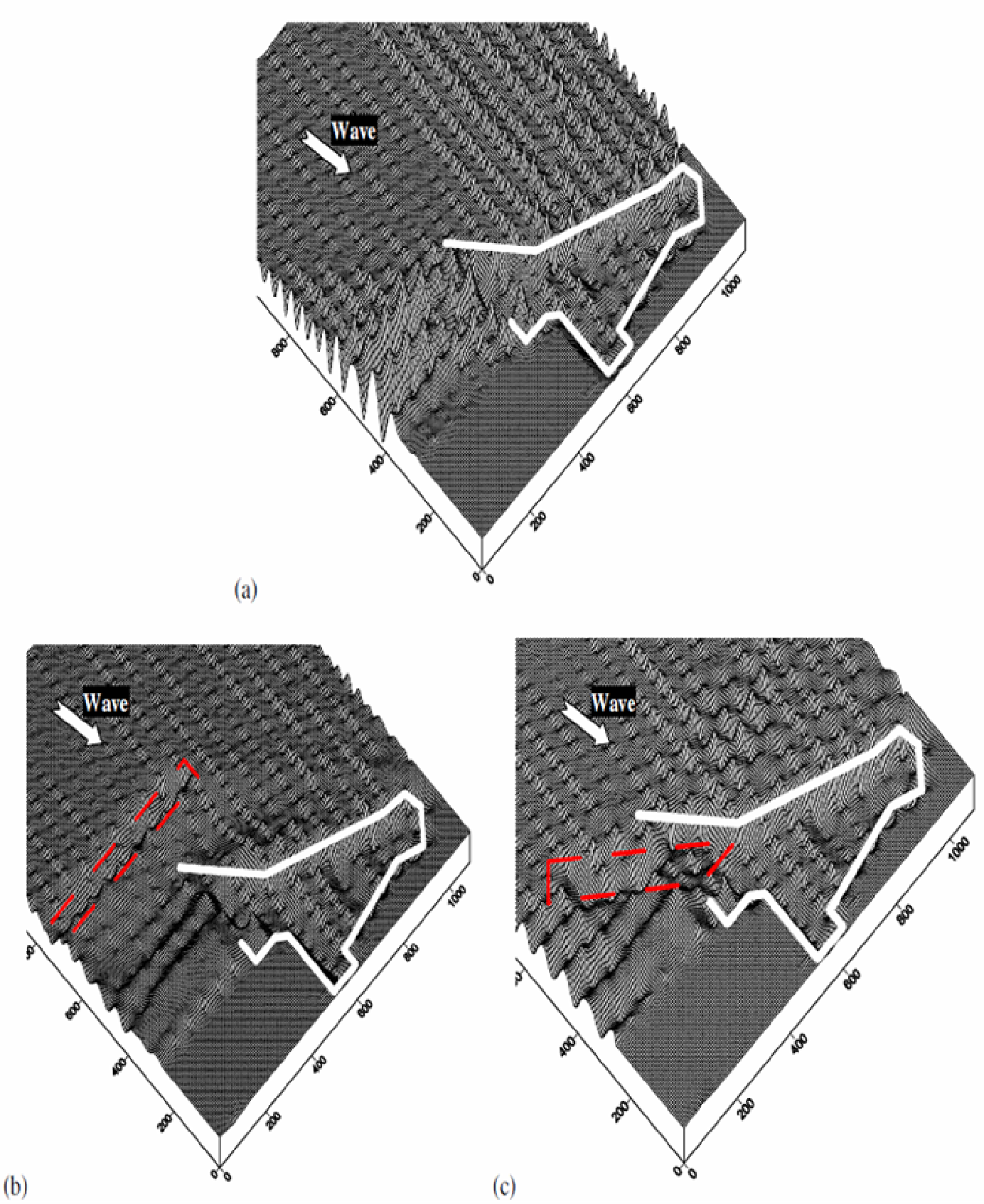

Figure 5. The three dimensional diffraction diagrams in Soma harbor for regular waves.

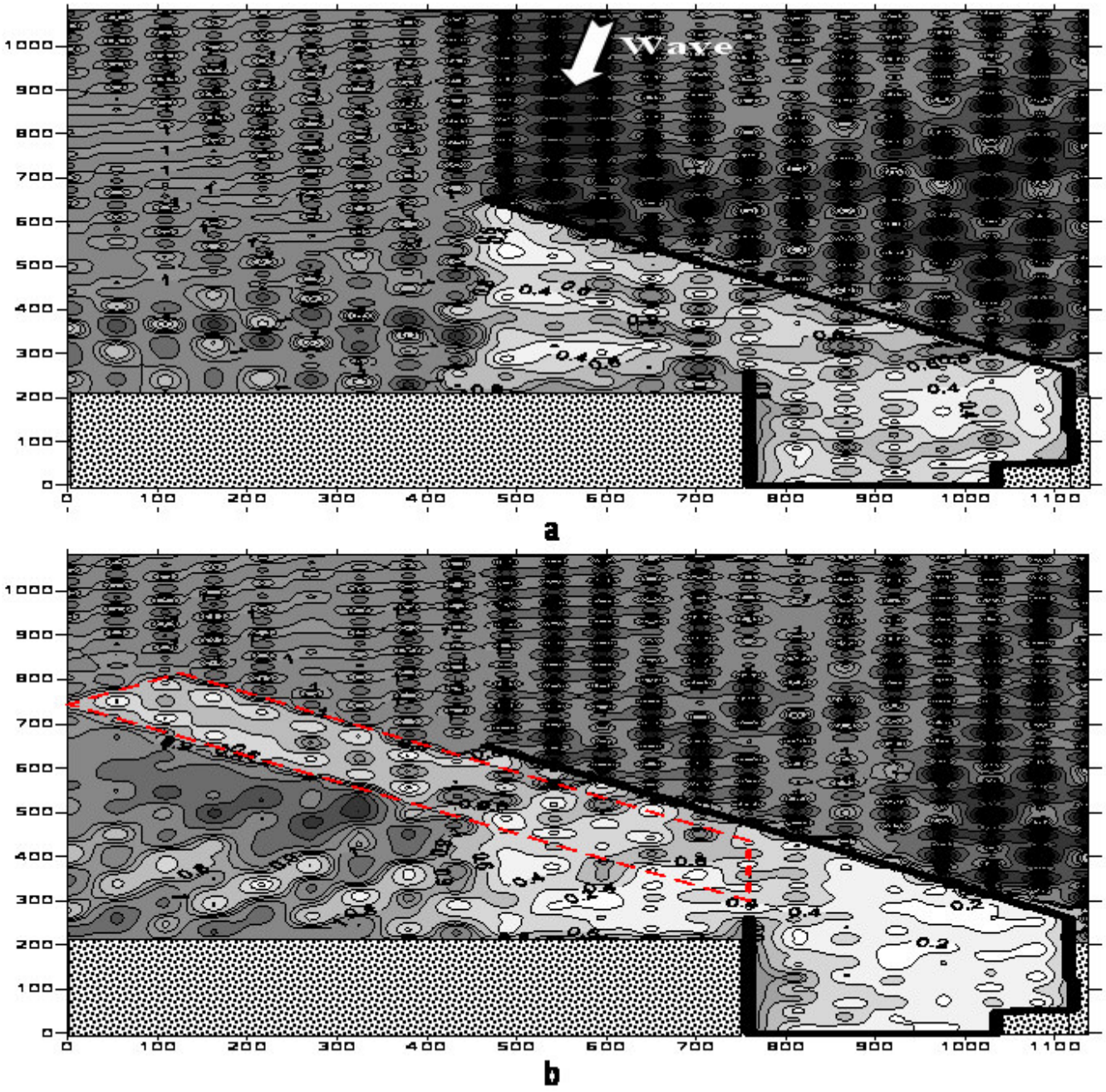

Figure 6. The diffraction contour plots in Kashima harbor for regular waves. (a) Without pit (b) entrance pit.

of regular waves in Kashima harbour obtained by the present numerical model. For the case without the pit in Figure 6(a), wave height is high and the wave crest is spiky at the front of the main breakwater. It makes high wave heights inside the harbour and causes high harbour oscillation.

For the case of entrance pit in Figure 6(b), the reduced wave from the edge of the front of the breakwater propagates into the harbour. It makes low wave height inside the harbour and there is still and weak oscillation within the harbour. Figure 7 displays the three dimensional diffraction diagram for regular waves in Kashima harbour. By placing a pit the waves are reduced from offshore, and then this subdued wave energy propagates into the harbour.

Analysis of random waves

Figure 8 shows results for the diffraction coefficient of

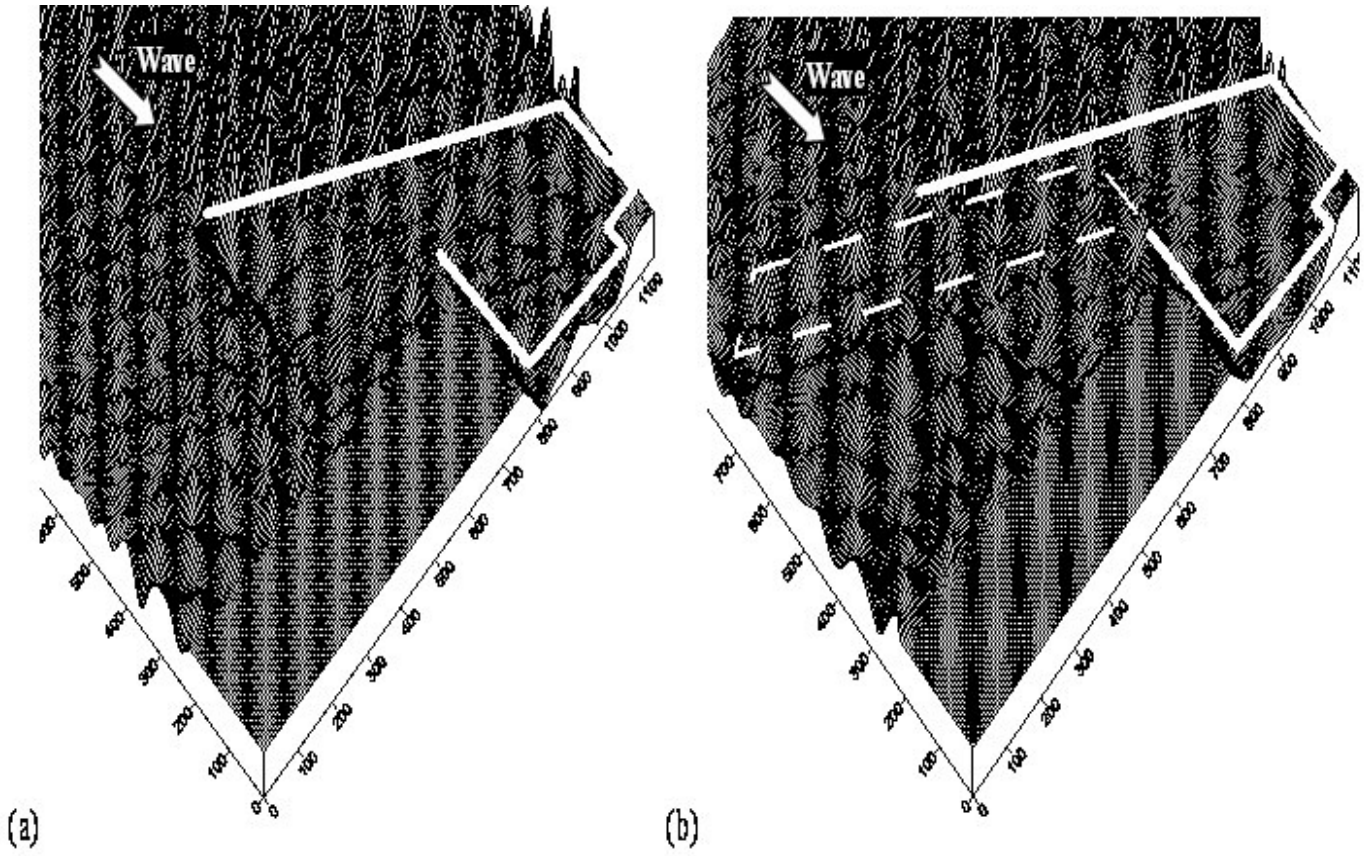

Figure 7. The three dimensional diffraction diagrams in Kashima harbor for regular waves.

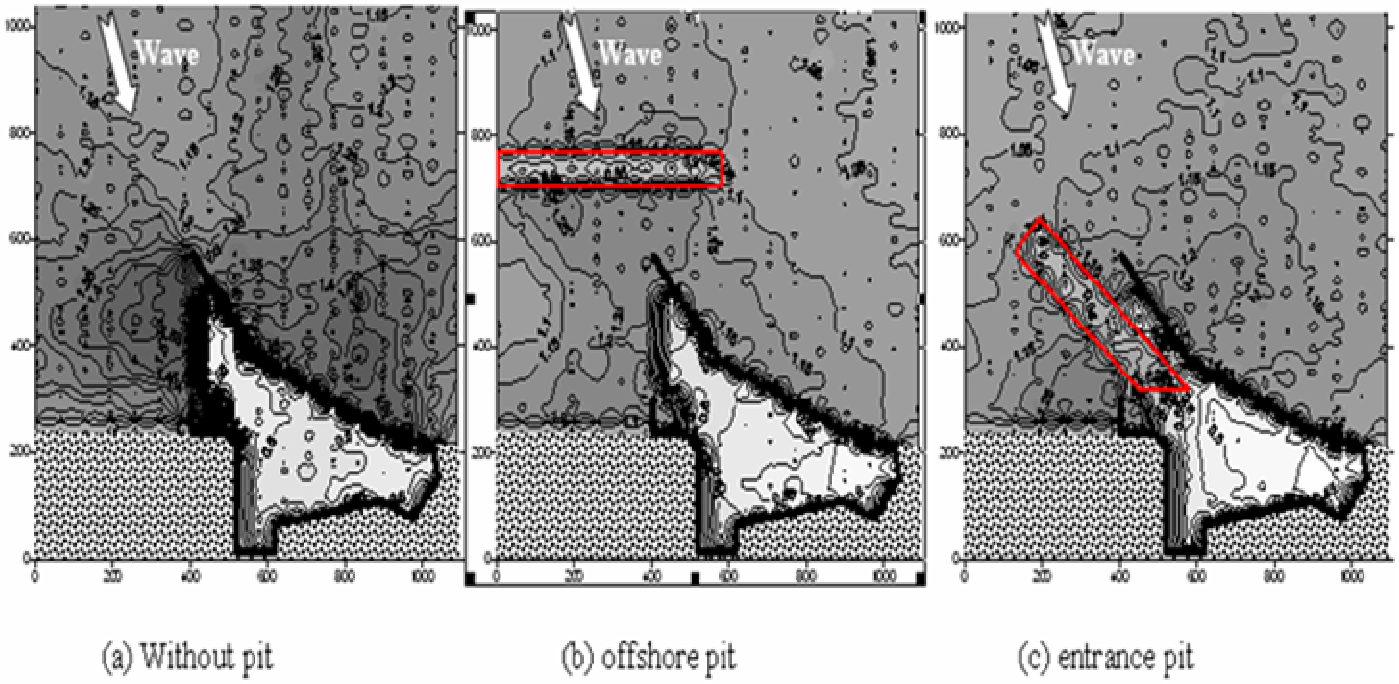

Figure 8. The diffraction contour plots in Soma harbor for random waves.

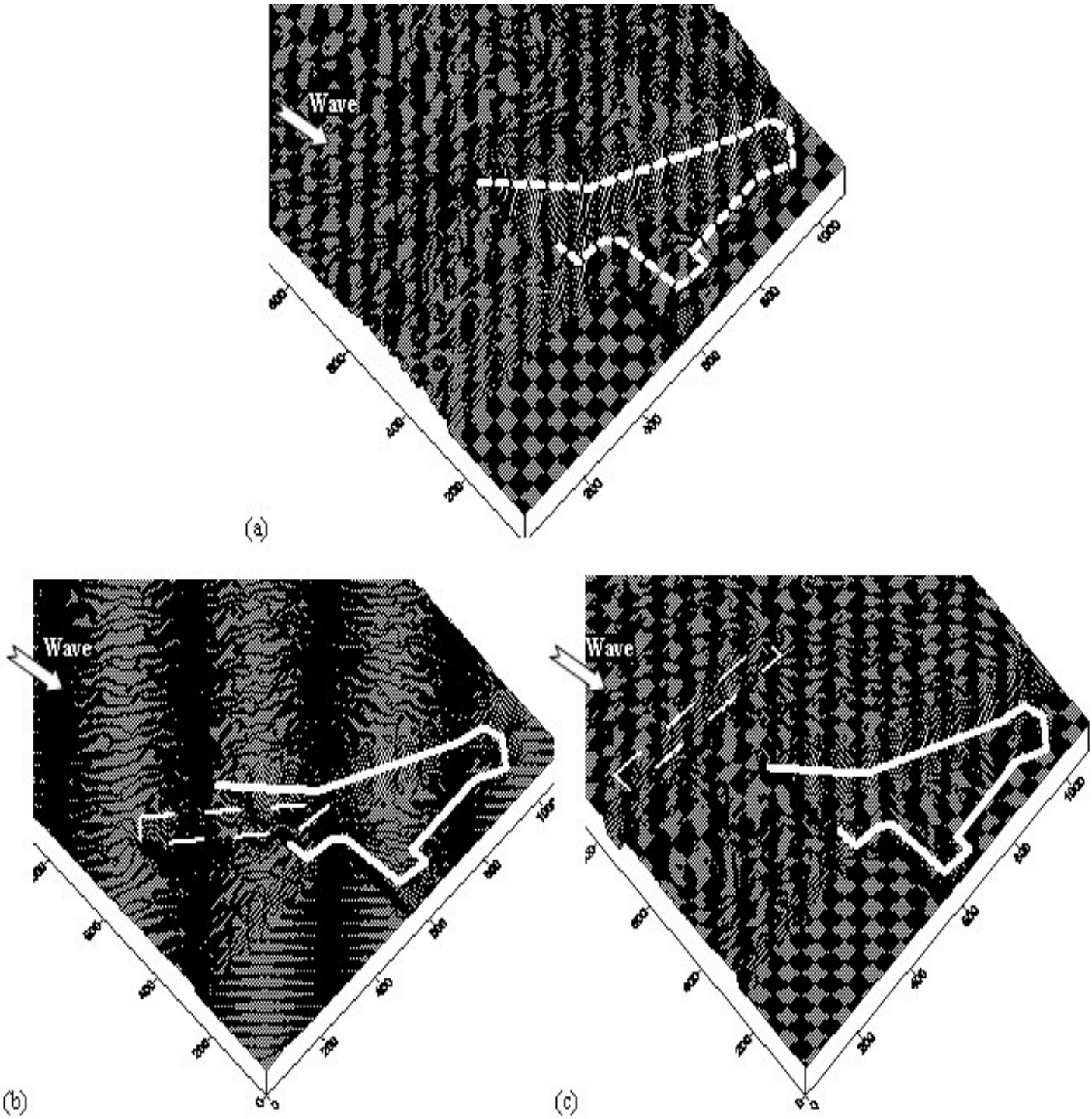

Figure 9. The three dimensional diffraction diagrams in Soma harbor for random waves.

random waves in Soma harbour obtained by the present numerical model. The random waves over the pit reduce wave energy and wave height is lower when there is a pit than where there is not a pit. The wave superposition is also reduced. And also the band width of low wave height behind the pit is distributed as a radial shape. It means that wave height is reduced at a broad range. Figure 9 display the three dimensional diffraction diagram for random waves in Soma harbour. Figure 10 shows results for the diffraction coefficient of random waves in Kashima harbour obtained by the present numerical model. Figure 11 display the three dimensional diffraction diagram for

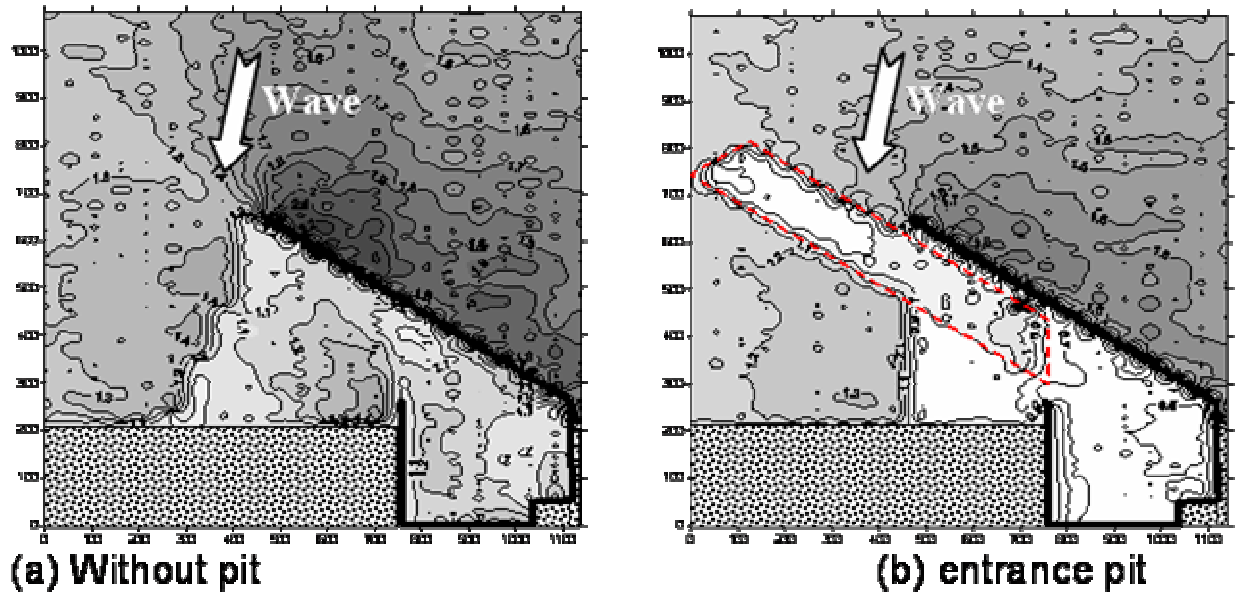

Figure 10. The diffraction contour plots in Kashima harbor for random wave.

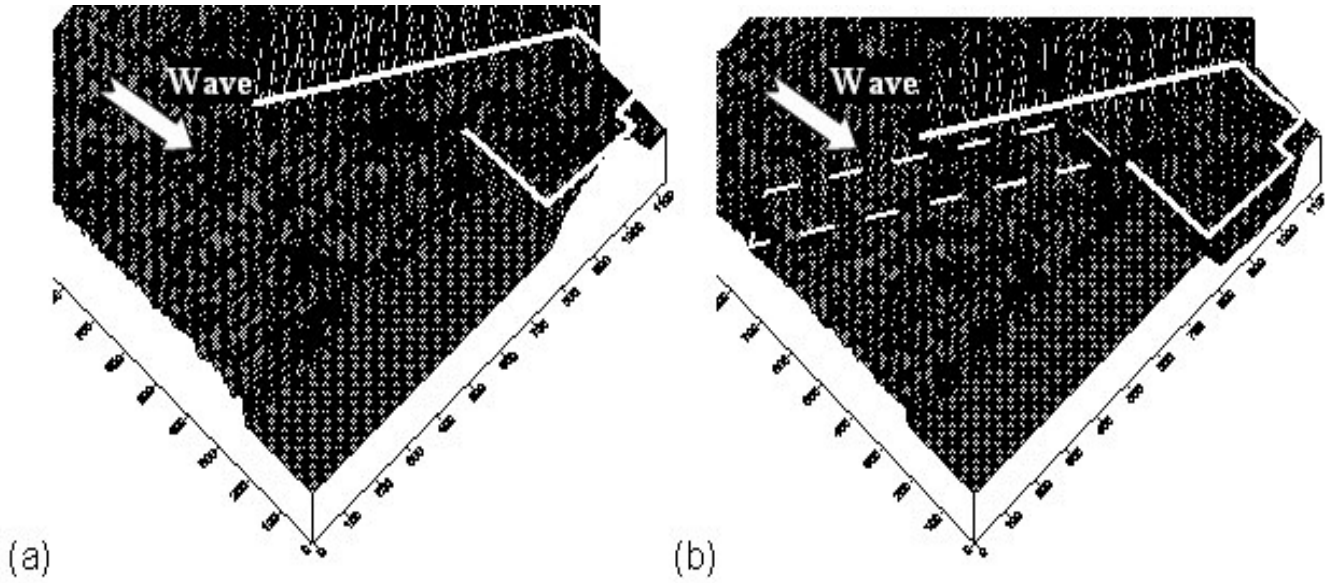

Figure 11. The three dimensional diffraction diagrams in Kashima harbor for random waves.

random waves in Kashima harbour.

Conclusion

The present study estimates the decreasing effects of diffracted wave fields in-and around selected harbours (Soma and Kashima harbours) including the region of the outer breakwater, when a navigation channel is dredgedat the vicinity of a harbour entrance. This study is about the composite interaction of the three problems: pit boundaries, depth discontinuity of pit, and harbor boundaries. The boundary conditions are established for those problems and applied to the boundary integral equation.

Results for the incident wave conditions have been presented to illustrate the wave height distribution inside the harbour and on the wave field by horizontal and oblique direction pit. The diffraction coefficients under the cases of regular waves and random waves are reduced first at the entrance of the harbor by a long pit, which controls the incident wave energy and affects it so that it

is then decreased when the wave propagates into the harbour. It is noticed that the results from the present numerical model accurately provides the diffracted wave height inside the harbour under the random-wave condition, when the navigation channel is dredged at the entrance of harbour. Thus, this may be extended to apply with confidence in harbour planning and design applications.

REFERENCES

Briggs MJ, Borgman Le, Bratteland E (2003). Probability assessment for deep-draft navigation channel design, Coastal. Eng., 48: 29-50.

Briggs MJ, Sargent F (2000). Evaluate and acquire inertial navigation system (INS). Unpublished technical note, U.S. Army Engineer Research and Development Center, Vicksburg, MS, Oct.

Goda Y (1985). Random seas and design of maritime structures. University of Tokyo Press, Tokyo, Japan.

Kennedy AB, Slatton KC, Starek M, Kampa K, Cho HC (2010). Hurricane response of nearshore borrow pits from airborne bathymetric lidar. J. Waterway, Port, Coastal. Ocean. Eng., 136(46): 46-58.

Kim SD (2007). Multidirectional random wave diffraction in a harbor with partial-reflecting boundary by placing submarine pit. PhD Thesis, Chung-Ang. University.

Kirby JT (2000). Analysis of regular and random ocean waves. Notes for cieg 681. Technical report, center for applied ocean research, University of Delaware.

Kirby JT, Dalrymple RA (1983). Propagation of obliquely incident water waves over a trench. J. Fluid. Mech., 133: 47-63.

Lee JJ, Ayer RM (1981). Wave propagation over a rectangular trench. J. Fluid. Mech., 110: 335-347.

McDougal WG, Williams AN, Furukawa K (1996). Multiple-pit breakwaters. J. Waterway, Port, Coastal. Ocean. Eng. ASCE, 122(1): 27-33.

Miles JW (1967). Surface-wave scattering matrix for a shelf. J. Fluid. Mech., 28: 755-767.

Mitsuyasu H (1970). Spectral development of wind generated waves. Proceedings of 17th Japanese Conference on Coastal Engineering, JSCE, Tokyo, Japan, 1-7 (in Japanese)

Mitsuyasu H, Tasai F, Suhara T, Mizuno S, Ohkusu M, Honda T, Rikiishi K (1975). Observation of the directional spectrum of ocean waves using a cloverleaf buoy. J. Phy. Oceanography. 5: 750-760.

Newman JN (1965). Propagation of water waves over an infinite step. J. Fluid Mech., 23: 399-415.

Ravens TM, Jepsen RA (2006). Computational fluid dynamics analysis of flow in a straight flume for sediment erodibility testing. J. Waterway, Port, Coastal, Ocean. Eng., 132: 457-461.

Reniers A, Roelvink D, Thornton E (2000). Morphodynamical modeling of an embayed beach under wave group forcing. Proceedings of 22th international conference of Coastal Eng., 3: 3219-3228.

Saito E, Oki M, Shimizu T, Ugai S, Isobe M (1993). On the characteristics of wave transformation by using a harbor model. Proceedings of 40th Japanese Conference on Coastal Engineering. JSCE, Tokyo, Japan. (in Japanese) pp. 56-60.

Takezawa M, Lee, HS, Lee BH, Kim IJ, Williams AN (2000). Diffraction of water waves due to a pit breakwater. Hydraulic Engineering Software VIII, WIT Press, UK, pp. 243-252.

Williams AN (1990). Diffraction of long waves by rectangular pit. J. Waterway, Port, Coastal . Ocean. Eng, ASCE, 116(4): 459-469.

Work PA, Fehrenbacher F, Voulgaris G (2004). Nearshore impacts of dredging for beach nourishment. J. Waterway, Port, Coastal, Ocean. Eng., 130: 303-311.